DOI: 10.6060/mhc161285b

Cytotoxicity of New Metal Porphyrinates Based on Chlorophyll *a* Derivatives

Y. I. Pylina,[a] D. M. Shadrin,[a] O. G. Shevchenko,[a] I. S. Khudyaeva,[b] D. V. Belykh,[b@] and I. O. Velegzhaninov[a]

[a]*Institute of Biology of Komi Scientific Centre of Ural Division RAS, 167982 Syktyvkar, Russia*
[b]*Institute of Chemistry of Komi Scientific Centre of Ural Division RAS, 167000 Syktyvkar, Russia*
[@]*Corresponding author E-mail: belykh-dv@chemi.komisc.ru, belykh-dv@mail.ru*

*Chlorophyll a derivatives are frequently used in photodynamic therapy of cancer. They are one of the prospective classes of compounds for screening of chemotherapeutic drugs with increased efficiency due to their malignant neoplasms affinity and dark cytotoxicity. The aim of the present work is to investigate some new porphyrinates of transition metals based on chlorophyll a and to reveal prospective cytostatic anticancer agents. A number of highly toxic compounds have been found. Mechanisms of biological activity of the most effective compound – Zn-13(1)-N-methylamide-15(2),17(2)-dimethyl ester of chlorin e_6 (**Zn-1**) have been studied. This compound has a threshold pattern of dose-effect relationship in both HeLa and A549 cells. This may be considered as an advantage which increases the efficiency in case of target delivery of the compound to the tumor. Fluorescence microscopy showed that compound **Zn-1** is able to penetrate rapidly into the cell. Caspase 3 activity analysis gives evidences of a remarkably early induction of apoptosis (within 3 h from the beginning of exposure). This is confirmed by the presence of separate pool of cells with highly fragmented DNA detected with Comet assay. Analysis of hemolytic activity in mice erythrocytes allows to suggest that biomembranes are the main targets of the **Zn-1** compound. Expressions of stress-response genes in HeLa cells after 8 h exposure to **Zn-1** indirectly confirms this hypothesis. Thus, new metalloporphyrins have been discovered and their bioactivity has been investigated in vitro.*

Keywords: Chlorophyll *a*, metalloporphyrin, cytotoxicity, anticancer agent.

Цитотоксичность новых порфиринатов металлов на основе производных хлорофилла *a*

Я. И. Пылина,[a] Д. М. Шадрин,[a] О. Г. Шевченко,[a] И. С. Худяева,[b] Д. В. Белых,[b@] И. О. Велегжанинов[a]

[a]*Федеральное государственное бюджетное учреждение науки Институт биологии Коми НЦ УрО РАН, 167982 Сыктывкар, Россия*
[b]*Федеральное государственное бюджетное учреждение науки Институт химии Коми НЦ УрО РАН, 167000 Сыктывкар, Россия*
[@]*E-mail: belykh-dv@chemi.komisc.ru, belykh-dv@mail.ru*

*Показано, что порфиринаты Zn, Cu и Ni на основе хлорина e_6 13-N-метиламида-15,17 диметилового эфира обладают высокой цитотоксичностью в экспериментах in vitro. Наиболее эффективное соединение – Zn-13(1)-N-метиламид-15(2),17(2)-диметиловый эфир хлорина e_6 (**Zn-1**) – было исследовано более подробно.*

Ключевые слова: Хлорофилл *a*, металлопорфирин, цитотоксичность, противораковый агент.

Introduction

Chemotherapy is one of the main approaches to treat oncological diseases, but the majority of anticancer drugs is very toxic and have a number of significant adverse effects. A possible way to minimize adverse effects is to develop chemotherapeutic agents with high tropism to malignant neoplasms. Porphyrins show a great potential for anticancer drug screening,[1] because of their dark cytotoxicity and significant photosensitizing properties.[2-6] Many compounds of this group also have high tropism to malignant neoplasms.[7,8] Photosensitizing properties are successfully used in photodynamic therapy of cancer.[9,10] But at the same time the clinical potential and the mechanism of dark cytostatic/cytotoxic activity of those compounds haven't been studied enough.

Photoinduced activity of porphyrins is supposed to be caused by their ability to turn into excited triplet-state under the light exposure and then to interact directly with biological macromolecules or transmit the energy to molecular oxygen converting it into excited singlet state.[11,12] Common targets of photosensitizers are plasmolemma, mitochondrions and lysosomes, but any lipids, proteins and nucleic acids also may be destroyed depending on the intracellular localization of the agent.[11,12] Physical and chemical mechanisms of dark cytotoxicity of porphyrins have not been completely studied and can probably be different for various compounds.

The present work aims to study dark cytotoxicity of chlorophyll *a* derivatives and porphyrinates of transition metals synthesized on their basis.

Experimental

Synthesis of compounds

Synthesis, purification and verification of the newly tested porphyrins and porphyrinates was performed as previously described in details.[13,14]

Cell culture and the algorithm of compounds testing

HeLa (cervical cancer), A549 (pulmonary adenocarcinoma) and HELF-104 (normal human embryonic lung fibroblasts, derived from an 8-week embryo) cell lines were purchased from "BioloT", St-Petersburg, Russia. Cells were cultured in DMEM/F12 medium (PAA Laboratories GmbH, Austria) supplemented with 10 % (v/v) fetal bovine serum (Thermo Scientific HyClone, UK) at 37 °C and 5 % CO_2. No antibiotics were used. Cells were subcultured two times a week using 0.05 % trypsin-EDTA solution (PanEco, Russia).

The fluorometric microculture cytotoxicity assay (FMCA)

Stock solutions of the 12 analyzed compounds were prepared by dissolving in dimethylsulfoxide (DMSO) (Amresco, USA) in different concentrations. One microliter of the stock solution of the tested compound was added in the corresponding concentration to 199 µl of the medium, containing 1000 cells of the HELF-104 line or 5000 cells of HeLa or A549 lines in sterile culture plates. The final concentrations of the compounds varied from 0.01 up to 100 µM while DMSO was always 0.5 % (v/v). The same concentration of DMSO was added to the reference samples. Etoposide (ICN Biomedicals Inc., USA) – a substance with known cytotoxic activity served as a positive control. Cells with the studied compounds were cultured for 8, 24, 48 or 72 h depending on the experiment at 37 °C, 100 % humidity and 5 % CO_2, in the dark. The amount of living cells was analyzed by fluorimetry.[15] A monolayer culture was washed with 200 µl of phosphate buffered saline (PBS) just after the medium had been removed. Then 100 µl of fluorescein diacetate (Sigma, USA) solution in FDA-buffer was added to each well for 40 min incubation at 37 °C / 5 % CO_2. All the manipulations were done under low light condition to avoid photoinduced effect. Fluorescence of the incubated solution was measured at excitation wavelength 485 nm and emission 520 nm (Fluorat-02 Panorama, Lumex, Russia). No detectable fluorescence was observed after incubation of fluorescein diacetate at 37 °C / 5 % CO_2 without cells. Amount of living cells was estimated as according to Lindhagen *et al.* (2008).[15] From nine to fifteen microcultures were separately treated and tested for each data point. Data were analyzed with Statistica 6.0 software (StatSoft Inc. USA) using Student's t-criterion, and checked for artefacts by Grabbs criterion. The probit analysis, implemented in SPSS 15.0 (SPSS Inc. USA) software, was used for calculating IC_{50}.

Estimation of compound Zn-1 ability to penetrate the plasmalemma

Compound **Zn-1** ability to penetrate into the cell was estimated using fluorescent microscopy. HeLa cells (5000 per well) were grown on a microscope slide with a 12 well silicone chamber (Ibidi GmbH, Germany) in 199 µl of DMEM/F12 medium containing 10 % (v/v) of fetal bovine serum. The cells were incubated with 1 µl of compound **Zn-1** solution in DMSO (final concentration of compound was 1 µM) for 30 min at 37 °C, 100 % humidity and 5 % CO_2. After incubation the medium with the studied compound and silicone chamber all were removed, cells were washed with PBS and covered with a cover glass. Images were captured using Axioscope A1 microscope with CCD camera AxioCam ICm 1 and an AxioVision software package (Carl Zeiss) under the transmitted light and fluorescent microscopy excitation wave 352–377 nm and emission >397 nm.

Comet-assay

The level of DNA damage was estimated using alkaline version of Comet-assay. HeLa cells (20000 cells per well) were incubated for 8 h with compound **Zn-1** (2.7 and 5 µM) or Etoposide (100 µM) in the sterile culture plates at 37 °C and 5 % CO_2. Pure DMSO (0.5 % (v/v)) was used as a negative control. After incubation the medium was removed, cells were washed with 200 µl of PBS and detached with 20 µl of trypsin-EDTA solution. After trypsinization 80 µl of medium was added and the resulting suspension was quickly mixed with 233 µl of 1 % low melting point agarose solution prepared in PBS. The obtained mixture was placed on slides (100 µl per slide), pre-coated with 1 % normal melting point agarose solution and covered with cover-slips. After a 5 min incubation at 4 °C, cover-slips were gently removed and slides were immersed into a lysis buffer (2.5 M NaCl, 100 mM Na_2EDTA, 10 mM Tris-HCl, p*H* 10.0, 10 % DMSO, 1 % Triton X-100) and incubated at 4 °C overnight. After the lysis the slides were put into alkaline solution (300 µM NaOH, 1 µM EDTA; p*H* 13.0) for DNA unwinding (40 min at +4 °C). Electrophoresis was done in the same alkaline solution for 25 min at 1 V/cm. Then the slides were washed for 15 min in neutralizing solution (0.4 µM Tris, 10 µM HCl; p*H* 7.5) and twice in distilled water for 7 min. Washed slides were placed in 95 % ethanol for 10 min and dried. The processed slides were then stained with 100 µl of Ethydium bromide (MERCK, Germany) (2 µg/ml) and covered with a cover glass. Images were captured using a fluorescent microscopy Axioscop A1 (Carl Zeiss, Germany) CCD camera AxioCam ICm 1 and an AxioVision

software package (Carl Zeiss). DNA damage level was assessed as Olive moment using CometScorePro (TriTekCorp, USA) software in a semi-automatic mode. From fifty to eighty cells per slide were analyzed. Six slides with separately treated cultures were made for each data point. Mean values of the median Olive moments were calculated for each slide. Mann-Whitney test was used to estimate the difference between the treatment variants.

Analysis of Caspase 3 activity

Caspase 3 Assay Kit Fluorimetric (Sigma, USA) was used to assess the induction of apoptosis. HeLa cells (15000 cells per well) were incubated for 3 or 24 h with compound **Zn-1** (1 and 2.7 μM) or with 100 μM Etoposide in sterile culture plates at 37 °C and 5 % CO_2. Pure DMSO (0.5 % (v/v)) was used as the reference sample. After incubation the medium was removed, cells were washed with 200 μl of PBS, and 25 μl of lysis solution from Caspase 3 AssayKit was added. Then standard protocol of the analysis was used. Fluorescence was measured on Fluorat-02 Panorama (Lumex, Russia). The difference between the values obtained for the wells with and without specific Caspase 3 inhibitor was calculated to estimate a degree of the specific substrate destruction. Data were normalized according to the DNA concentrations in the corresponding lysates measured with PicoGreen® (Molecular Probes, Eugene, USA). The results were presented in pmol of the digested labeled substrate per amount of sample containing 1 ng of DNA. Six separately treated cultures were used for each data point. Two technical repeats were performed for each biological replicate. Data were averaged hierarchically.

Analysis of stress-response genes expression

HeLa cells ($4 \cdot 10^5$ per well) were incubated for 8 h with compound **Zn-1** (1 and 2.7 μM) in 6-well sterile culture plates at 37 °C and 5 % CO_2. Cell suspension with pure DMSO (0.5 % (v/v)) was used as the reference sample. After incubation medium was removed, cells were washed with 200 μl of PBS, and 350 μl of lysis solution from Aurum Total RNA MiniKit (Bio-Rad, USA) was added. Then RNA was extracted according to the manufacturer's protocol. Experiments were made in 3 parallel biological replications and 3 qPCR reactions within each replication. The quantity and quality of the total extracted RNA was estimated with the Experion automated electrophoresis system (Bio-Rad, USA). Reverse transcription was made with Maxima First Strand cDNA Synthesis Kit (Thermo Scientific, Rockford, IL, USA) according to the manufacturer's protocol. Real-time PCR was carried out using CFX96 PCR Detection System (Bio-Rad). Sequences of primers (Table 1) were taken from articles or developed with Primer BLAST online service. Primers' specificity was validated by examining melting curves using High Resolution Melt analysis mode and software for CFX96 PCR Detection System (Bio-Rad). Reaction mixture (20 μl) contained 20 ng of cDNA, primers (300 nM) and Maxima SYBR Green qPCR Master Mix (Thermo Scientific). The following PCR cycling conditions were used: 95 °C for 10 min, 40 cycles of 95 °C for 15 s, 60 °C for 60 s. Relative expression was calculated using the ΔCt method by normalizing to the housekeeping genes *ACTB* and *GAPDH*. Data were analyzed using CFX Manager (Bio-Rad), following statistical manipulations were done using Statistica 6.0 (StatSoft Inc. USA) and Excel (Microsoft). Data were checked for artefacts by Grabbs criterion. Statistical significance of the effects was estimated with one-way ANOVA with post-hoc Neuman-Keuls test.

Hemolytic activity and induction of latent changes in erythrocyte membranes

Analysis of hemolytic activity of compound **Zn-1** was made using erythrocyte suspension of *Mus musculus* L. blood. Erythrocytes were separated from plasma and other blood cells by centrifugation for 5 min and then washed 3 times with PBS (p*H* 7.4). Concentrated red cells obtained from 3–6 female outbred mice were combined and mixed. Analyses were performed in 5–7 separately treated aliquots of suspensions per each data point. All manipulations were done under low light condition to avoid photoinduced effect.

The compound solution in acetone was added to erythrocyte suspension in PBS (p*H* 7.4) and incubated 3 or 5 h at 37 °C in the thermostatic shaker Biosan ES-20 (Latvia). Concentrations 0.1, 1, 2.7, 5 and 10 μM of compound **Zn-1** were studied. Reference samples contained acetone (0.1 % v/v). Positive control sample with complete hemolysis was prepared using hypotonic condition (nonionic water). After incubation 1.5 ml of suspension were centrifuged (5 min, 1600 g) and the degree of hemolysis was estimated as a level of the hemoglobin in supernatant using spectrophotometer Spectronic Genesys 20 (Thermo, USA) at λ=541 nm. Hemolysis degree (A) was calculated by the equation (a) as a ratio of the real sample hemolysis (B) to a complete sample hemolysis (C).

$$A = \frac{B}{C} \cdot 100\ \%, \qquad (a)$$

where B is the optical density of the tested sample's supernatant and C is the optical density of the supernatant of the sample with complete hemolysis.

The sensitivity to nonionic detergent Triton X-100 after **Zn-1** treatment was studied to assess how **Zn-1** induced latent changes in erythrocytes' membranes. Triton X-100 (Ferak Berlin,

Table 1. Primer sequences for qRT-PCR analysis.

Gene	Forward Primer	Reverse Primer	Source
BAX	AGAGGATGATTGCCGCCGT	CAACCACCCTGGTCTTGGAT	[16]
BBC3	CTGTGAATCCTGTGCTCTGC	TCCTCCCTCTTCCGAGATTT	[16]
TNFSF10	GCTGAAGCAGATGCAGGACAAG	CTGACGGAGTTGCCACTTGAC	[17]
CDKN1A	CAGCAGAGGAAGACCATGTG	GGCGTTTGGAGTGGTAGAAA	[18]
CDKN2A	GACATCCCCGATTGAAAGAA	TTTACGGTAGTGGGGGAAGG	Primer BLAST*
SOD2	GCTGACGGCTGCATCTGTT	CCTGATTTGGACAAGCAGCAA	[19]
GSR	ATCCCCGGTGCCAGCTTAGG	AGCAATGTAACCTGCACCAACAA	[20]
PBP74	TCTGGACTGAATGTGCTTCG	ATCCCCATTTGTGGATTTCA	[21]
GAPDH	ACACCCACTCCTCCACCTTTG	GCTGTAGCCAAATTCGTTGTCATAC	[17]
ACTB	GCGCGGCTACAGCTTCA	CTTAATGTCACGCACGATTTCC	[22]

*Developed using Primer BLAST online service: http://www.ncbi.nlm.nih.gov/tools/primer-blast/

Germany) was added to the suspension as a 0.5 % solution in PBS (final concentration was 0.003 %) 1 h after **Zn-1** (1 and 2.7 μM) treatment as described above. Then cells were incubated during 5 h. Reference samples were incubated with **Zn-1** or Triton X-100 only. The spontaneous hemolysis level was measured simultaneously. The ability of compound **Zn-1** to change erythrocyte sensitivity to Triton X-100 was estimated by the interaction coefficient (Kw) calculated using the equation (b).[23]

$$Kw = \frac{I(X1, X2)}{I(X1, 0) + I(0, X2)}, \quad \text{(b)}$$

where $I(X1,X2)$ is the difference between hemolysis degree of the combined action (of **Zn-1** and Triton X-100) and the spontaneous level; $I(X1,0)$ is the difference between hemolysis level under compound **Zn-1** and the spontaneous level; $I(0,X2)$ is the difference between hemolysis level under Triton X-100 and the spontaneous level.

*Assessment of **Zn-1** ability to oxidize hemoglobin*

An absorption spectrum of hemolysates of the experimental and reference samples was analyzed using Fluorat-02 Panorama (Lumex, Russia) within the range 350–640 nm to assess **Zn-1** capability to oxidize hemoglobin. Shifting of Soret band (407 nm) was determined and the optical absorption value was measured.[24] Ratios of different hemoglobin forms (oxyHb, metHb and ferrylHb) were also calculated using extinction coefficients.[25]

Results

New chlorophyll a derivatives and their cytotoxicity

Chlorophyll *a* derivatives (structures are presented in Figure 1) were synthesized as it has been previously described.[13,14]

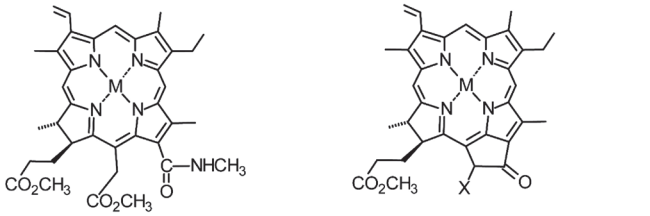

Figure1. Structures of chlorophyll *a* derivatives and porphyrinates of transition metals based on them. Reference designations are given in parentheses.

The correlation between HeLa cells survival rate and the tested compounds concentration (within the range from 0.01 μM to 100 μM) has been defined to estimate dark cytotoxicity of the new chlorophyll *a* derivatives (**1-3**) and porphyrinates of Cu, Ni and Zn synthesized on their base (Table 2). The compound **1**, that has no exocycle in its structure, has been found to be the most toxic among the three metal free chlorophyll *a* derivatives (**1-3**). The presence of the amide group at the position 13(2) of the exocycle results in the compound **3** toxicity increase compared to the compound **2** which has no amide group. In order to assess the affect of insertion of the metal cation into coordination sphere of chlorin we estimated the cytotoxicity affect for Cu, Ni and Zn complexes of compounds **1-3**. **Cu-2** and **Cu-3**; **Ni-2** and **Ni-3** compounds have minimal cytotoxicity among porphyrinates (at 100 μM the survival index is more than 50 %).

All the Zn porphyrinates have been found to be highly cytotoxic (Table 2). This could have been caused by the extracoordination ability of the Zn porphyrinates. Also Zn complexes of similar macrocycles are reported[6] to be highly toxic. The most toxic metal-free compound **1** and its zinc-containing derivative (**Zn-1**) showed a small difference in IC_{50}, but **Zn-1** was significantly more toxic in 10 μM concentration (the average cell survival indexes were 23.8 and 3.64, $p=1.2\cdot10^{-5}$).

An interesting peculiarity has been found in the relation between the concentration of porphirinates and their toxic effect. Cancer cell survival rate decreases from about 100 % at 1 μM of **Zn-1** and **Zn-2** down to complete cell elimination at 10 μM. The similar effect has been found for **Cu-1** and **Ni-1**, but the sharp change in toxicity was observed between 10 and 100 μM. The properties found together with the possible affinity of porphyrins to malignant neoplasms can increase efficiency of anticancer therapy, which can be used in probable drug investigation.

To detailize the threshold dependency of the toxic effect on concentration of **Zn-1**, **Cu-1** and **Ni-1** compounds additional tests were made. Etoposide was used as a standard cytotoxic agent (Figure 2). Two cancer cell lines (HeLa and A549) and normal human lung fibroblasts cell line (HELF-104) on the 22–24 passage were used for the following experiment.

A threshold dependency of the cytotoxic effect on concentration was found for all three porphyrinates of the compound **1**. The sharp change in the toxic effect from minimal values up to complete cell elimination

Table 2. The ability of the new compounds and Etoposide to inhibit the growth of HeLa cells after 72 h incubation, expressed as IC_{50}.

Compound	IC_{50}, μM	95 % Confidence Limits, μM
1	2.66	1.82–3.91
2	>100	–
3	13.72	5.66–45.36
Zn-1	2.36	2.13–2.57
Zn-2	5.98	5.03–7.26
Zn-3	2.46	0.73–9.89
Cu-1	7.24	6.63–7.87
Cu-2	>100	–
Cu-3	>100	–
Ni-1	9.90	9.32–10.50
Ni-2	>100	–
Ni-3	>100	–
Etoposide	0.28	0.19–0.41

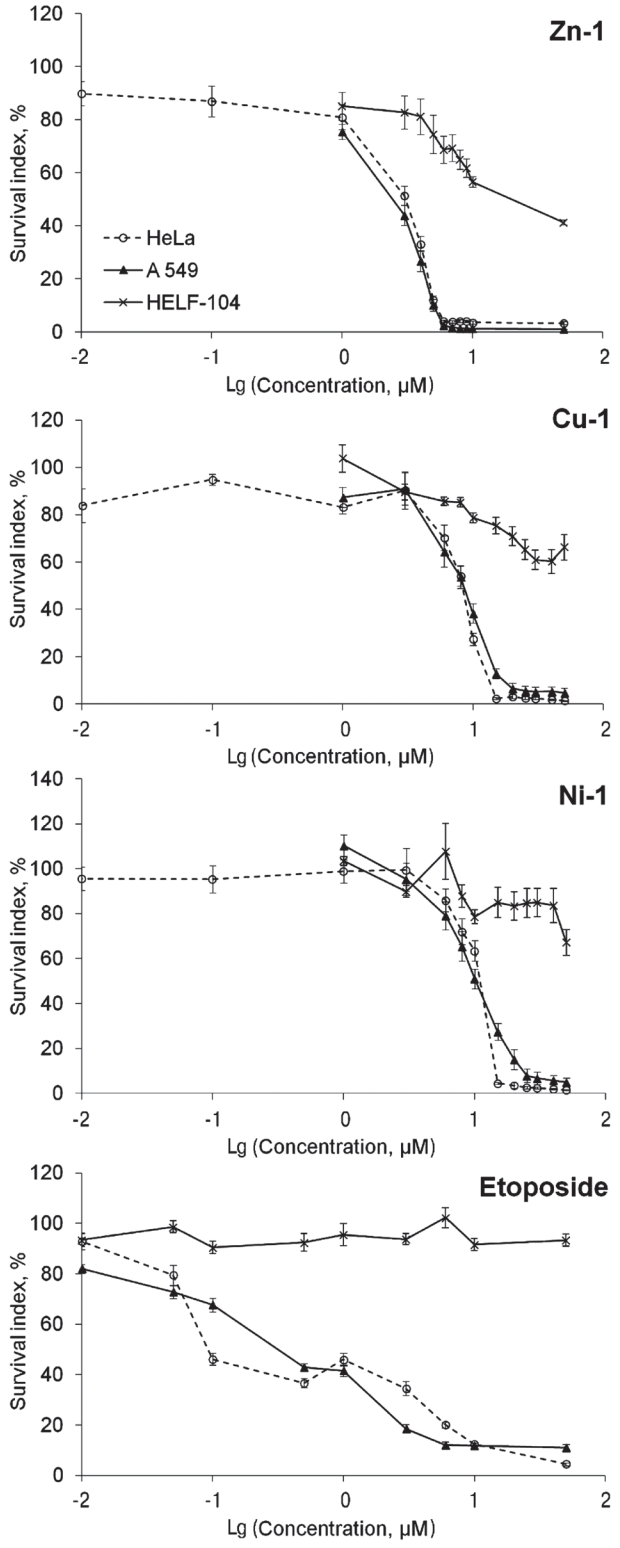

Figure 2. Survival rate of HeLa, A549 and HELF-104 cell lines estimated with FMCA after 72 h exposure of the compounds studied (average value obtained using 9–15 separately treated microcultures are presented with SEM).

was observed in a narrow concentration range. The highly toxic porphyrinate **Zn-1** showed the most drastic threshold effect.

All three metalloporphyrins were found to be less toxic in case of normal not immortalized fibroblasts HELF-104 as compared with HeLa, A549 cells within the experimental conditions presented. The half maximal inhibitory concentrations of **Zn-1**, **Cu-1** and **Ni-1** for A549 cells were 2.54, 7.62 and 9.66 μM correspondingly. At the same time for fibroblasts **Zn-1** IC_{50} value was 28.2 μM and for **Cu-1** and **Ni-1** the same values were higher than 100 μM. Etoposide exposure during 72 h resulted in no decrease in the number of fibroblasts in microcultures. Most likely this is a result of slow proliferation of HELF-104 cells, because Etoposide toxicity was established only after 144 h of incubation (IC_{50}≈44.4 μM).

Zn-1 was studied in detail, because it is highly toxic and has a small interval between toxic and non-toxic concentrations.

*The ability of **Zn-1** to penetrate the plasma membrane*

Porphyrinates autofluorescence was used to estimate the ability of **Zn-1** to penetrate the plasmalemma and the following potential to destroy intracellular structures. Analysis of the fluorescence spectrum of 0.5 μM water-DMSO solution prepared the same way as for biotests showed that maximum photon emission was observed at 642 nm, provided that the exciting wave was lower than 440 nm (with maximums at 410 and 320 nm) (Figure 3A,B). This allows to assess **Zn-1** accumulation in the cells using fluorescent microscopy (Figure 3). Cells incubation for 30 min in growth medium containing 1 μM of **Zn-1** resulted in their fluorescence in the red spectral region. Fluorescence was not distributed evenly in the cell. The cytoplasm was stained more than the nucleus. The fluorescence was not observed if the cells were incubated in the same growth medium with DMSO but without **Zn-1**. Thus **Zn-1** is able to quickly penetrate the cell membrane and thus can affect intracellular structures.

*The genotoxic and apoptosis-inducing activity of **Zn-1***

Alkaline version of Comet assay, detecting single and double-stranded breaks and alkali-label sites in DNA was used to test DNA damage induction with 2.7 and 5 μM of **Zn-1** in HeLa cells. The concentration of 2.7 μM was chosen as IC_{50} calculated based on preliminary data (final calculated IC_{50} is 2.36 μM). It is also important to note that **Zn-1** in 2.7 μM concentration did not cause massive cell death after 8 h of incubation (more than 80 % cells were alive as was estimated by FMCA), whereas 5 μM concentration decreases the amount of viable cells by 81 % relative to control. This lethal concentration of **Zn-1** (5 μM) induced more DNA damage than 100 μM of the Etoposide (Figure 4). But the distribution of cells according to the degree of DNA damage was different. Treatment with Etoposide which is known to induce DNA damage[26] led to an increased number of moderately damaged cells. That is why frequency distribution had a maximum at the lowest values and a gradual decrease of the damage degree (Figure 4). Treatment with **Zn-1**, on the contrary, led to an emergence of strongly damaged cells registered as an additional maximum on the frequency distribution diagrams.

It is believed that apoptotic cells are visualized by Comet assay as “comets” in which most of DNA migrates

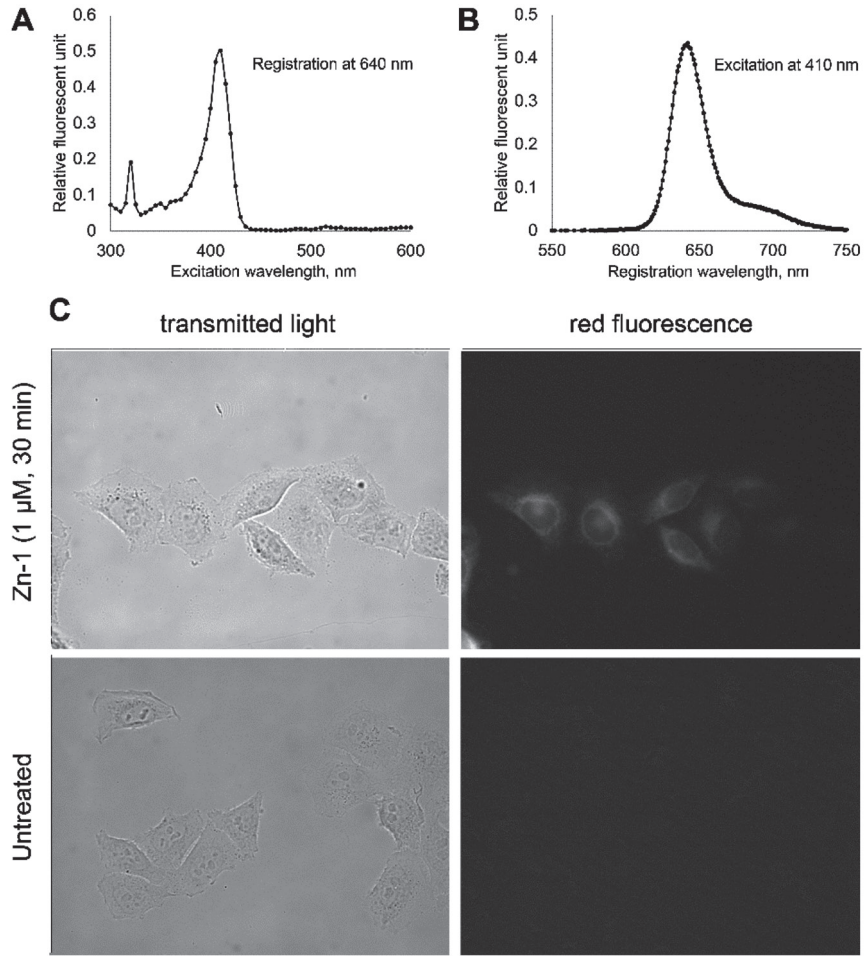

Figure 3. Spectra of fluorescence excitation (A) and emission (B) of 0.5 μM **Zn-1** solution. Light micrographs (C, left column) and fluorescent micrographs (C, right column) of cells after 30 min treatment with **Zn-1** (C, upper row) and without it (C, lower row). Magnification: 600×.

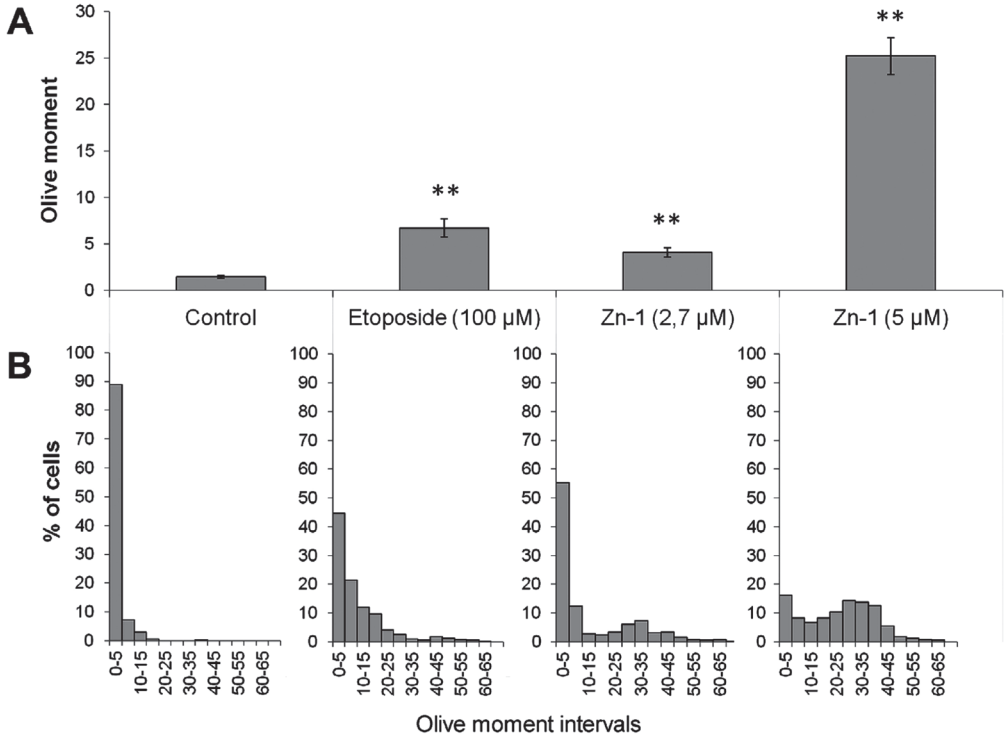

Figure 4. The level of DNA damages after **Zn-1** and Etoposide treatment assessed by the Comet-test.
A – Olive moment mean values; B – frequency distribution diagrams. Mean values are calculated from more than 300 cells (>50 cells in each of 6 separately treated replicates) per treatment. ** – difference from control value is significant at $p<0.005$ (Mann-Whitney test).

into the "tail".[27,28] Thus an appearance of the pool of strongly fragmented nucleoids can be considered to be a result of high frequency apoptosis. At the same time a slight increase in moderately damaged nucleoids after **Zn-1** treatment indicates that the compound can induce DNA damage directly or indirectly.

Analysis of the Caspase 3 activity provides an evidence (Figure 5) of apoptosis induction as well. Caspase 3 activity increased significantly after three h of treatment with **Zn-1** in the concentrations of 1 and 2.7 μM. 24-h **Zn-1** treatment resulted in decrease of the Caspase 3 activity below the spontaneous level. This may be due to the rapid death of the most sensitive cell fraction. Exposure of cells to higher concentrations of **Zn-1** for 24 h led to an almost complete cell death and their washout by the medium prior to analysis. Data normalization was not possible in that case because DNA concentration was on the level of the noise signal. FMCA assay 24 h after treatment of the cells with 5 μM **Zn-1** showed an almost 20-fold drop in fluorescence, which indicated a respective reduction of the mass of viable cells (data not shown).

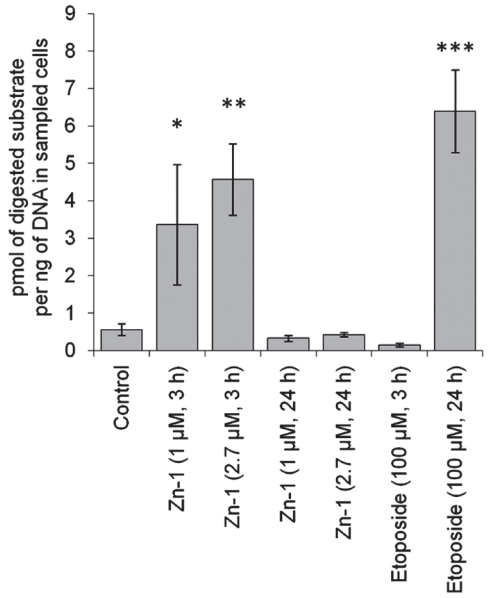

Figure 5. Caspase 3 activity after 3 and 24 h of treatment with **Zn-1** (1 and 2.7 μM) and Etoposide (100 μM). Mean values of 6 separately treated replicates (each obtained from two technical replicates) are presented with SEM. Differences from control values are significant at * – $p<0.05$; ** – $p<0.005$; *** – $p<0.001$.

Treatment with the Etoposide – a well-known apoptosis inductor,[29,30] caused no apoptosis after 3 h but resulted in Caspase 3 activity increase after 24 h (Figure 5).

*Expression of stress responsive genes under **Zn-1***

The gene expression analysis was performed to study the stress-response of HeLa cells after an 8 h incubation with **Zn-1**. It is known, that in the period from 4 to 24 hours after the impact of the stress factor, the maximum development of the stress response at the level of gene expression is observed. Results of many experimental studies show it.[31-35] Thus, 8 h were enough to alter gene expression, but not enough to induce the massive cell death using **Zn-1** in concentrations 1-5 μM. Genes with a definite function and a proved mRNA level reaction to different chemical and physical stress factors were selected. After treatment with **Zn-1** a slight trend to activation of the transcription of *BAX* and *BBC3* genes was found (Figure 6). These genes encode the proteins which play the key role in apoptosis induction by mitochondrial membrane permeabilization.[36,37]

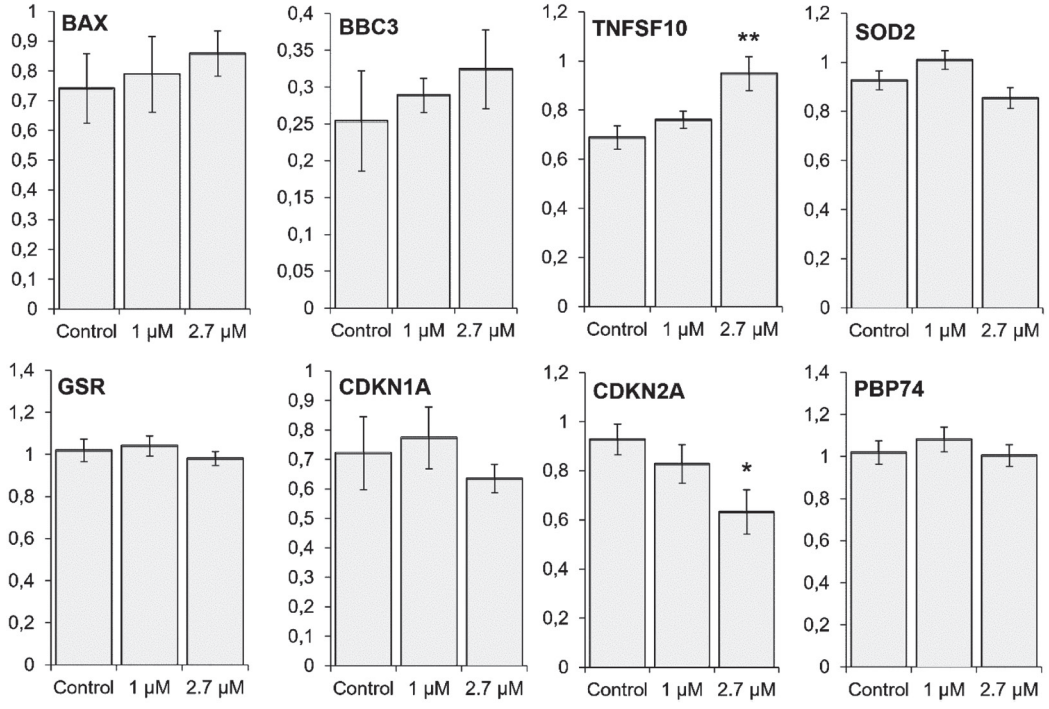

Figure 6. Expression of stress responsive genes in HeLa cells after 8 h treatment with 1 and 2.7 of **Zn-1**. Mean values of 9 replications (3 biological × 3 technical) are presented with SEM. * and ** denote statistically significant effect of **Zn-1** treatment with $p<0.01$ and $p<0.001$ respectively (ANOVA with post-hoc analysis by Newman-Keuls test).

A significant increase in expression of *TNFSF10* which functions mainly as a proapoptosis ligand was also observed.[38] Activation of *BAX*, *BBC3* and *TNFSF10* gives an evidences of progressing transcriptional proapoptosis response. However, most cells apparently die earlier because of the rapid apoptosis which develops at posttranscriptional level.

The expression of the key stress-reactive regulator of the cell-cycle[39-41] – cycline-dependent kinases *p21* (*CDKN1A*) – did not change after 8-h of treatment with **Zn-1**, while *p16* (*CDKN2A*) expression even decreased. This indicates an absence of activation of another defense strategy – cell cycle arrest in G1-S checkpoint. Moreover there were no changes in mRNA levels of antioxidant system genes, which usually increase in oxidative stress conditions: *SOD2* (encodes the mitochondrial enzyme detoxifying superoxide radicals[42]) and *GSR* (encodes the glutathione reductase[43]). Expression of *PBP74*, encoding the multifunctional member of Heat shock proteins 70 family (Mortalin), did not change either.[44]

*The effect of **Zn-1** on murine erythrocytes*

The toxicity of **Zn-1** to murine erythrocytes has been studied because all the data obtained suggest that biomembranes could be the main targets of **Zn-1** toxic effect.

A significant hemolytic activity of **Zn-1** after 3 and 5-h of contact with murine erythrocyte suspension started at the concentration of 5 μM. The two-fold increase of the concentration resulted in 90 % cell death (Figure 7). Analysis of the erythrocyte's hemolysates absorption spectrum of the reference and experimental sample showed that adding **Zn-1** resulted in no change in the position of the Soret band (407 nm) and no decrease in optical absorption in this region of the spectrum. That indicates an absence of **Zn-1** interactions with the hemoglobin.[24] Similar values of absorption at 560, 577 and 630 nm showed that the reference and experimental samples have the same contents of native and oxidized hemoglobin forms. So metHb/oxyHb and ferrylHb/oxyHb relations were 0.569±0.026 and 0.138±0.001 in intact erythrocytes, and 0.491±0.033 and 0.140±0.004 respectively in the cells treated with the porphyrinate.

Experiments with a nonionic detergent Triton X-100 which is widely used as an agent for biomembrane destabilization[45] were made to detect any hidden changes in erythrocyte membrane structure under **Zn-1** which was used in the concentrations that do not produce significant hemolysis (1 and 2.7 μM). After the treatment with **Zn-1** for 1 h, Triton X-100 was added into the control and experimental erythrocyte suspensions and then the cell death dynamics was assessed (Figure 7). At the same time

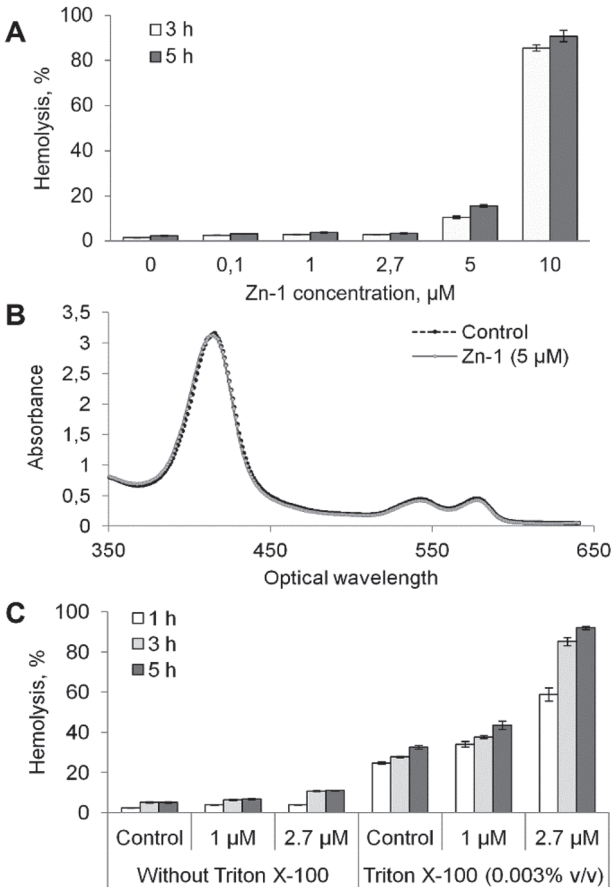

Figure 7. The effect of **Zn-1** on murine erythrocytes. The degree of erythrocyte's hemolysis after 3 and 5 h of incubation with 0.1–10 μM of **Zn-1** (A). The absorbance spectrum of the control erythrocyte's hemolysates and after 5 h of incubation with 5 μM of **Zn-1** (lines are identical) (B). The hemolysis degree of the of erythrocytes treated with Triton X-100 added after a 1 h incubation with 1 and 2.7 μM **Zn-1** (the duration of the experiment was 1, 3 and 5 h) (C). Mean values of 5–7 separately treated replicates are presented with SEM.

the hemolysis level was estimated in the samples not treated with Triton X-100, which allowed to calculate[23] the interaction coefficient (Kw) of the two factors (Table 3). Analysis of the data presented indicates the synergistic action of Triton-X-100 and **Zn-1** (Kw values are significantly greater than 1).

Discussion

The new highly cytotoxic chlorophyll *a* derivatives were presented in this work. Some of them were characterized

Table 3. Interaction coefficients (Kw) of Triton-X-100 and **Zn-1**.

Incubation time, h	Coefficient of interaction	
	Triton X-100 (0.003% v/v) and **Zn-1** (1 μM)	Triton X-100 (0.003% v/v) and **Zn-1** (2.7 μM)
1	1.32***	2.36***
3	1.31***	2.83***
5	1.32*	2.61***

Interaction coefficient (Kw) differs from 1 at *p<0.05, ***p<0.001.

by the gradual and others by the sharp increase in cytotoxic effect with the concentration enhance. Compounds **1**-**3** had significant differences in dark cytotoxic activity (Table 2). The most toxic compound **1** did not contain the exocycle, in contrast to compounds **2** and **3**. The two last compounds had differences by presence of the amide group at the position 13(2) of the exocycle. The mechanisms of the dark cytotoxic activity of porphyrin derivatives are still unclear. Among the expected targets in the studies, there are DNA,[46] membrane structures[47] and individual signaling cascades, for example, a disruption of the interaction of MDM2 and p53 proteins.[48] At the same time, there are hypotheses about the effect on the dark activity of compounds to the nature and quantity of substituents on the periphery of the macrocycle and the presence or absence of an exocycle.

Therefore, data presented in this article and the listed researches do not contain the direct evidence of any mechanism and possible causes of differences in the dark toxicity of the studied compounds That is why we focused on investigating the toxicity mechanism of compound **Zn-1**, which was found as the most toxic among the compounds tested.

The results of Comet assay performed on HeLa cells give an evidences that **Zn-1** induces DNA damage as many other porphyrins do.[6,49] A number of strongly degraded nucleoids resulted in the additional maximum in the frequency distribution diagram by Olive moment. This observation also indirectly indicates apoptosis activation (Figure 4). The ability to induce apoptosis is confirmed by the Caspase 3 activation in HeLa cells after 3 h of incubation with **Zn-1** (Figure 5). Such a rapid activation of apoptosis was not observed after the treatment with Etoposide (Figure 5), the main effect of which is the induction of DNA double-strand breaks.[30] In the latter case, activation of apoptosis was the result of DNA-damage signal. Differences in the rate of Caspase 3 activation may indicate the different mechanisms for **Zn-1**-induced and Etoposide-induced apoptosis. It is known that the inner pathway of the apoptosis can be initiated by different signal sources within the cell (damaged DNA, activated oncogenes,[50] injured endoplasmic reticulum;[51] inhibited microtubule[52] and others) and through various signal cascades which finally start mitochondria or lysosomes permeabilization. This permeabilization releases the factors activating caspase-dependent or caspase-independent apoptosis.[50,53,54] Mitochondrial outer membrane permeabilization determines the point-of-no-return of the most if not all the signal-transduction cascades leading to apoptosis.[54] The fact of fast apoptosis activation caused by **Zn-1** together with its ability to damage membranes and quickly penetrate into the cell support the suggestion that **Zn-1** can interact directly with mitochondrial membrane. This can results in permeabilization and fast activation of caspases. Some compounds are known to have the ability to permeabilize mitochondrial outer membrane without upstream signaling and without any effect on *BAK* and *BAX* enzymes activity.[55,56] This assumption is consistent with the concept according to which apoptosis is the primary mechanism of cell death if mitochondria is the target of dark or photo-induced toxicity effect. Whereas if the main target is the plasma membrane or lysosomes, the cells die mainly because of necrosis.[57,58] Presumably, **Zn-1** can induce the damage of all the membrane structures of cells and provoke apoptosis as well as necrosis.

This suggestion is also supported by the presence of slight changes in mRNA expression of genes, known to be induced in response to DNA damage. So, only slight changes in expression of proapoptotic genes *BAX*, *BBC3* and *TNFSF10* was found after 8 h of treatment with **Zn-1** in HeLa cells. Unchanged or even decreased expression level of the cell cycle controlling genes (*CDKN1A* and *CDKN2A*) gives an evidence of the absence of the cell cycle checkpoint activation. Invariable expression of genes coding free radical detoxification enzymes (*SOD2* and *GSR*) and Mortaline in HeLa cells together with the absence of hemoglobin oxidation in murine erythrocytes all indicate the non-oxidative properties of the **Zn-1** toxic activity.

Significant interaction of **Zn-1** with cell membrane was found in the experiments on murine erythrocytes: high hemolysis level (Figure 7A,B) was opposed to the absence of hemoglobin oxidation. In addition, a brief contact of erythrocytes with the studied porphyrinates leads to emergence of the hidden changes in plasmalemma. It was found in the experiments with the nonionic detergent Triton X-100, which decreases the level of molecular packing by incorporation into the lipid bilayer. This leads to an increase of phospholipid hydrocarbon chains mobility and results in the membrane permeability and hemolysis.[59] High degree of acyl chain packing is the determinant factor of the resistance of membrane to the action of Triton X-100 in erythrocytes.[60] Increased sensitivity of **Zn-1** treated erythrocytes to Triton X-100 found in our experiments could be the result of changes in the structure of the membrane lipid phase.

Taking in to account the found properties, it is unlikely, that the compound **Zn-1** has a high potential as an independent chemotherapeutic agent. Therefore, the threshold dependency of the toxic effect on concentration, the ability to rapidly penetrate the interior of the cell and induce apoptosis, allow **Zn-1** to be considered as a potential effector molecule for targeting tumor delivery using nanoparticle and monoclonal antibody technology.

Conclusions

Thus, both the nature of the metal cation and the ligand structure can impact the dark toxicity of porphyrinates based on chlorophyll *a* derivatives. Potential antineoplastic cytostatics have been revealed among the studied compounds and the biological activity of the most active one of them, **Zn-1**, has been investigated. It has been found that **Zn-1** quickly penetrates the cells, affects the membrane and induces the caspase-dependent apoptosis. Early apoptosis induction accompanied with the slight or absent changes in DNA-damage gene expression can be explained by the direct mitochondrial membrane damage by **Zn-1**. The new compound shows the sharp dose dependence and the threshold dose dependence of the toxic effect. This may be considered as an advantage which increases the efficiency in case of target delivery of the compound to the tumor.

Acknowledgements. This work was supported by the Russian Scientific Foundation (Grant number 15-13-00096 RSF). We thank Elena S. Belykh for help in writing the manuscript.

References

1. Senge M.O. *Photodiagn. Photodyn. Ther.* **2012**, *9*, 170–179.
2. Moan J., Berg K. *Photochem. Photobiol.* **1992**, *55*, 931–948.
3. Lipson R.L., Baldes E.J., Gray M.J. *Cancer* **1967**, *20*, 2255–2257.
4. Pope A.J., MacRobert A.J., Phillips D., Bown S.G. *Br. J. Cancer* **1991**, *64*, 875–879.
5. Songca S.P. *J. Pharm. Pharmacol.* **2001**, *53*, 1469–1475.
6. Wongsinkongman P., Brossi A., Wang H-K., Bastow K.F., Lee K-H. *Bioorg. Med. Chem.* **2002**, *10*, 583–591.
7. Ackroyd R., Kelty C., Brown N., Reed M. *Photochem. Photobiol.* **2001**, *74*, 656–669.
8. Ali H., Lier J.E. *Chem. Rev.* **1999**, *99*, 2379–2450.
9. Filonenko E.V., Sokolov V.V., Chissov V.I., Lukyanets E.A., Vorozhtsov G.N. *Photodiagn. Photodyn. Ther.* **2008**, *5*, 187–190.
10. Shlakhtin S.V. and Trukhacheva T.V. *Vestnik pharmacii* **2010**, *48*, 1–20.
11. Castano A.P., Demidova T.N., Hamblin M.R. *Photodiagn. Photodyn. Ther.* **2004**, *1*, 279–293.
12. Dougherty T.J. *Photochem. Photobiol.* **1987**, *45*, 879–889.
13. Mazaletskaya L.I., Sheludchenko N.I., Tarabukina I.S., Belykh D.V. *Petroleum Chemistry* **2014**, *54*, 309–315.
14. Tarabukina I.S., Pylina Y.I., Velegzhaninov I.O., Startceva O.M., Shadrin D.M., Belykh D.V. *Butlerov Commun.* **2015**, *43*, 18–23.
15. Lindhagen L., Nygren P., Larsson R. *Nat. Protoc.* **2008**, *3*, 1364–1369.
16. Sharma A.K., Ali A., Gogna R., Singh A.K., Pati U. *PLOS One* **2009**, *4*, e7159.
17. Cheng K.C., Huang H.C., Chen J.H., Hsu J.W., Cheng H.C., Ou C.H., Yang W.B., Chen S.T., Wong C.H., Juan H.F. *BMC Genomics* **2007**, *8*, 411.
18. Ghosh S., Krishna M. *Mutat. Res*. **2012**, *729*, 61–72.
19. Marconett C.N., Zhou B., Rieger M.E., Selamat S.A., Dubourd M., Fang X., Lynch S.K., Stueve T.R., Siegmund K.D., Berman B.P., Borok Z. and Laird-Offringa I.A. *PLOS Genetics* **2013**, *9*, e1003513.
20. Corrales R.M., Galarreta D., Herreras J., Calonge M., Chaves F. *Can. J. Ophthalmol.* **2007**, *1*, 35–39.
21. Bian Q., Fernandes A.F., Taylor A., Wu M., Pereira P., Shang F. *Mol. Vis.* **2008**, *14*, 403–412.
22. Ding K-K., Shang Z-F., Hao C., Xu Q-Z., Shen J-J., Yang C.J., Xie Y.H., Qiao C., Wang Y., Xu L.L., Zhou P.K. *Radiat. Environ. Biophys.* **2009**, *48*, 205–213.
23. Geras'kin S.A., Kim J.K., Dikarev V.G., Oudalova A.A., Dikareva N.S., Spirin Y.V. *Mutat. Res.* **2005**, *586*, 147–159.
24. Vardapetyan H.R., Martirosyan A.S., Tiratsuyan S.G., Hovhannisyan A.A. *J. Photochem. Photobiol. B: Biol.* **2010**, *101*, 53–58.
25. Berg J.M., Kamp J.A.F., Lubin B.H., Roelofsen B., Kuypers F.A. *Free Radical. Biol. Med.* **1992**, *12*, 487–498.
26. Maanen J.M.S. van, Retel J., de Vries J., Pinedo H.M. *JNCI: Journal of the National Cancer Institute* **1988**, *80*, 1526–1533.
27. Olive P.L., Frazer G., Banáth J.P. *Radiat. Res.* **1993**, *136*, 130–136.
28. Fairbairn D.W., Olive P.L., O'Neill K.L. *Mutat. Res.* **1995**, *339*, 37–59.
29. Montecucco A., Biamonti G. *Cancer Lett.* **2007**, *252*, 9–18.
30. Kaufmann S.H. *Biochim. Biophys. Acta* **1998**, *1400*, 195–211.
31. Murray J.I., Whitfield M.L., Trinklein N.D., Myers R.M., Brown P.O., Botstein D. *Mol. Biol. Cell* **2004**, *15*, 2361–2374.
32. Echchgadda I., Roth C.C., Cerna C.Z., Wilmink G.J. *Cells* **2013**, *2*, 224–243.
33. Ding L.H., Shingyoji M., Chen F., Hwang J.J., Burma S., Lee C., Cheng J.F., Chen D.J. *Radiat. Res.* **2005**, *164*, 17–26.
34. Fischer B.M., Neumann D., Piberger A.L., Risnes S.F., Köberle B., Hartwig A. *Arch. Toxicol.* **2016**, *90*, 2745–2761.
35. Sokolov M.V., Panyutin I.V., Panyutin I.G., Neumann R.D. *Mutat. Res., Fundam. Mol. Mech. Mutagen.* **2011**, *709–710*, 40–48.
36. Westphal D., Kluck R.M., Dewson G. *Cell Death and Differentiation* **2014**, *21*, 196–205.
37. Hikisz P., Kiliańska Z.M. *Cell. Mol. Biol. Lett.* **2012**, *17*, 646–669.
38. Azahri N.S.M., Kavurma M.M. *Cell. Mol. Life Sci.* **2013**, *70*, 3617–3629.
39. Sancar A., Lindsey-Boltz L.A., Unsal-Kacmaz K., Linn S. *Annu. Rev. Biochem.* **2004**, *73*, 39–85.
40. Rayess H., Wang M.B., Srivatsan E.S. *Int. J. Cancer* **2012**, *130*, 1715–1725.
41. Carnero A., Hannon G.J. The INK4 Family of CDK Inhibitors. In: *Current Topics in Microbiology and Immunology* (Vogt P.K., Reed S.I., Eds.) Berlin, Heidelberg: Springer-Verlag, **1998**. p. 43–55.
42. Candas D., Li J.J. *Antioxid. Redox Signaling* **2014**, *20*, 1599–1617.
43. Zhu H., Cao Z., Zhang L., Trush M.A., Li Y. *Mol. Cell. Biochem.* **2007**, *301*, 47–59.
44. Flachbartova Z., Kovacech B. *Acta Virologica* **2013**, *57*, 3–15.
45. Findlay J.B.C., Evans W.H. *Biological Membranes: A Practical Approach.* IRL Press: Oxford, **1987**.
46. Dutikova Yu.V., Ol'shevskaya V.A., Shtil A.A., Kaluzhny D.N. *Russ. J. Biotherapy* **2011**, *4(*10), 47–53.
47. Belykh D.V., Shevchenko O.G., Tarabukina I.S. *Macroheterocycles* **2014**, *7*, 79–87.
48. Zawacka-Pankau J., Krachulec J., Grulkowski I., Bielawski K.P., Selivanova G. *Toxicol. Appl. Pharmacol.* **2008**, *232*, 487–497.
49. Tovmasyan A., Babayan N., Poghosyan D., Margaryan K., Harutyunyan B., Grigoryan R., Sarkisyan N., Spasojevic I., Mamyan S., Sahakyan L., Aroutiounian R., Ghazaryan R., Gasparyan G. *J. Inorg. Biochem.* **2014**, *140*, 94–103.
50. Hassan M., Watari H., AbuAlmaaty A., Ohba Y., Sakuragi N. *Biomed Res. Int.* **2014**, http://dx.doi.org/10.1155/2014/150845.
51. Logue S.E., Cleary P., Saveljeva S., Samali A. *Apoptosis* **2013**, *18*, 537–546.
52. Muscarella D.E., Bloom S.E. *Toxicol. Appl. Pharmacology* **2008**, *228*, 93–104.
53. Johansson A.C., Appelqvist H., Nilsson C., Kågedal K., Roberg K., Ollinger K. *Apoptosis* **2010**, *15*, 527–540.
54. Perfettini J.L., Roumier T., Kroemer G. *Trends Cell Biol.* **2005**, *15*, 179–183.
55. Qian W., Salamoun J., Wang J., Roginskaya V., van Houten B., Wipf P. *Bioorg. Med. Chem. Lett.* **2015**, *25*, 856–863.
56. Huang W., Tang S., Qiao X., Ma W., Ji S., Wang K., Ye M., Yu S. *Fitoterapia* **2014**, *94*, 36–47.
57. Kassel D., Luo Y. *J. Photochem. Photobiol.* **1998**, *42*, 89–95.
58. Copley L., van der Watt P., Wirtz K.W., Parker M.I., Leaner V.D. *Int. J. Biochemi. Cell Biol.* **2008**, *40*, 227–235.
59. Preté P.S.C., Domingues C.C., Meirelles N.C., Malheiros S.V.P., Goñi F.M., de Paula E., Schreier S. *BBA- Biomembranes* **2011**, *1808*, 164–170.
60. Rodi P.M., Trucco V.M., Gennaro A.M. *Biophys, Chem.* **2008**, *135*, 14–18.

Received 12.12.2016
Accepted 10.02.2017